Supporting Information for

Multifunctional Pathology-mapping Theranostic Nanoplatform for US/MR Imaging and Ultrasound Therapy of Atherosclerosis

Binyang Gao [a, b], Jinshun Xu [a, b], Jie Zhou [a, b], Huan Zhang [a, b], Xinrui Yang [a, b], Hong Wang [a, b], Jianbo Huang [b], Feng Yan [b, **], Yan Luo [a, b, *]

[*] Corresponding author. *E-mail address: luoyanddoc@163.com (Yan Luo)*

[**] Corresponding author. *E-mail address: yan_feng@scu.edu.cn (Feng Yan)*

1. Supplementary Methods

Synthesis of the MPmTNs

The double emulsification (W/O/W) method was used to synthesize the Fe-PFP-PLGA NPs, as previous study reported [1, 2]. Briefly, 50 mg of PLGA was fully dissolved in 2 mL of dichloromethane (CH_2Cl_2) as the organic phase, 40 μL of Fe_3O_4 and 200 μL of PFP were added as the inner aqueous phase. The mixture was vibrated acoustically for 3 min (5 s on and 5 s off) with a power of 8 % of 750 W via an ultrasonic oscillation instrument (SCIENTZ-IID, Ningbo Scientz Biotechnology Co., Ltd., Zhejiang, China). After the first emulsion, 6 mL of 4 % PVA solution was poured into above solution as the outer aqueous phase and emulsified for 5 min (5 s on and 5 s off) to produce a brown solution. Next, 10 mL of 2 % isopropanol solution was added and magnetically stirred constantly for 3 h until the organic solvents volatilized completely and the surface of the NPs solidified. Finally, the Fe-PFP-PLGA NPs were rinsed with double-distilled water three times to remove the unreacted materials, diluted to 10 mL and stored at 4 ℃ for further use. The entire fabrication process was conducted under ice-bath condition.

For the preparation of MPmTNs (aka 'the Fe-PFP-PLGA@PP1-cRGD NPs'), the carbodiimide-mediated amide bond formation method was used through following

steps [3, 4]. First, the Fe-PFP-PLGA NPs were centrifuged at 10 000 rpm for 10 min and resuspended by 10 mL 0.1 M MES buffer solution (pH=5.2) containing appropriate amount of EDC and NHS at a molar ratio of 2:1. The suspension vigorously stirred for 1 h to activate carboxyl groups of PLGA. Then, 10 mL of 0.1 M MES buffer solution (pH=8) was used to dissolve the mixture again after centrifugation, followed by the addition of 2 mg of PP1 peptides and 2 mg of cRGD peptides. The resulting solution was allowed to react for 12 h with a shaker. Finally, MPmTNs were rinsed with double-distilled water three times to remove the unreacted materials and diluted to 10 mL for further use. The entire fabrication process was conducted under ice-bath condition.

All types of NP were prepared using the same procedure described above. For the control NPs, PFP was replaced with doubled-distilled water in equal volume to form the Fe-PLGA NPs or the Fe-PLGA@PP1-cRGD NPs. The Fe-PFP-PLGA@PP1 NPs or the Fe-PFP-PLGA@cRGD NPs were synthesized without adding corresponding peptides. Fluorescently labeled NPs were prepared by introducing an appropriate amount of Dio (green) when dissolving PLGA in CH_2Cl_2.

Physical and Chemical Characterization of the NPs

Zeta potential (ζ), size, and polydispersity index (PDI) of different NPs were determined using a dynamic light scattering detector (DLS, Brookhaven Omni, Brookhaven Instruments Inc., Holtsville, NY, USA) at 25 ℃. Their internal structures were observed by transmission electron microscopy (TEM, Tecnai G2 F30 S-TWIN, FEI Co., Ltd., Hillsboro, Oregon State, USA). To further verify the loading and distribution of Fe_3O_4, PFP and peptides in the MPmTNs, a high-resolution image and elemental mapping images of iron (Fe), fluorine (F) and sulfur (S) were obtained by using a high-resolution TEM (HR-TEM, Talos F200X, FEI Co., Ltd., Hillsboro, Oregon State, USA). Fe concentration was quantitatively measured by an inductive coupled plasma emission spectrometer (ICP, ICPOES730, Agilent Technologies Inc., Santa Clara, California, USA). To test the stability, NPs were stored in phosphate-buffered saline (PBS) at 4℃ for 14 days, and measured the dynamic parameters of sizes and PDI at 0.5, 1, 2, 4, 8, 24, 48, and 336 h.

***In Vitro* Multimodal Imaging Property of MPmTNs**

To observe the multimodal imaging property of MPmTNs, the phase-transition process of PFP was first tested *in vitro*. 2 mL of 2 mg/mL MPmTNs were placed in a tissue mimicking phantom made of 3 % agarose gel and exposed to an ultrasonic therapeutic instrument (Sonic-Stimu Pro UT1041, Dundex Co., Ltd., Shenzhen, Guangdong, China) at 3 MHz, 30 % duty cycle and a power density of 1, 2 or 3 W/cm^2 for 1, 2 or 3 min, respectively. Immediately after ultrasonic irradiation, the samples were observed under an optical microscope (AX10 Imager A2/AX10 CAM HRC, Carl Zeiss, Co., Ltd., Jena, Germany), and the NPs were closely inspected for expansion, fusion, and conversion from liquid particles to gas microbubbles. On this basis, the optimal conditions of phase transition induced by ultrasonic irradiation are determined.

The subsequent ultrasound (US) imaging performance was further test *in vitro*. MPmTN was added to an agarose gel phantom and ultrasonic exposure at 3 W/cm^2, 3 MHz and 30 % duty cycle for 3 min by an ultrasonic therapeutic instrument (Sonic-Stimu Pro UT1041, Dundex Co., Ltd., Shenzhen, Guangdong, China). In the control groups, MPmTN was replaced with saline, the Fe-PLGA@PP1-cRGA NPs or the Fe-PFP-PLGA NPs, following the similar operations and conditions. Furthermore, the time-point experiment was conducted to explore optimal irradiation conditions, and MPmTN was exposed upon 3 W/cm^2, 3 MHz and 30 % duty cycle for 0, 2, 3, 4, 5, and 6 min. After exposure in each group, US images were collected immediately in conventional B mode (B-mode) and contrast-enhanced ultrasound mode (CEUS) using an ultrasound machine (iU22, Koninklijke Philips N.V., Eindhoven, NL). The acoustic intensities of the US images were analyzed using Image J software [5]. The region of interest (ROI) comprised uniform pixels.

To detect the MR imaging property *in vitro*, MPmTN were diluted with double-distilled water to create various iron concentrations. Considering the loading rate of Fe, the NPs theoretical concentrations of 0.82, 1.63, 2.45, 3.27, 4.08 mg/mL were respectively equivalent to iron concentrations of 0, 0.2, 0.4, 0.6, 0.8, 1.0 mM. Then, T_2-weighted

images were performed by an nuclear magnetic resonance (NMR) imaging system (MesoMR12-060H-I, Suzhou Niumag Analytical Instrument Co., Suzhou, Jiangsu, China) with the following parameters: 0.5 T coil; multi-slice spin echo (MSE) sequence; spectrometer frequency (SF), 12 MHz; echo time (TE), 60 ms; repetition time (TR), 400 ms; field of view (FOV), 100 mm and slice width, 6 mm. The T_2 values were obtained by an NMR analysis system (PQ001, Suzhou Niumag Analytical Instrument Co., Suzhou, Jiangsu, China) with the following parameters: 0.5 T coil; inversion recovery (IR) sequence; SF, 18 MHz; receiver bandwidth (SW), 200 KHz; radio frequency delay (RFD), 0.08 ms; TE 0.2 ms; number of echoes (NECH), 8000. A linear fit was conducted to analyze the correlation between the Fe concentration and the transverse relaxation rates ($R_2 = 1/T_2$).

Cell Culture and Activation

Lipopolysaccharide (LPS)-activated RAW 264.7 cells could highly express SR-A proteins on cell membranes, and thus they were widely used as cell model to simulate the macrophages in plaque sites. RAW 264.7 cells were purchased form Cellcook (Guangzhou Cellcook Cell Biotechnology, LTD., Guangzhou, China). The cells were cultured in Dulbecco's modified Eagle's medium supplemented with 10 % fetal bovine serum, using 25 cm^2 cell-culture flasks with a humidified atmosphere containing 5 % carbon dioxide (CO_2) at 37℃. The cells in the logarithmic growth phase could be used for experiments. The cells were activated with 100 ng/mL lipopolysaccharide (LPS) for 24 h.

Western Blot Analysis

To confirm the transdifferentiation and validate the expression of SR-A on the surface of macrophages, activated and unactivated cells were harvested for western blot (WB) analysis. Protein concentrations were determined with a bicinchoninic acid (BCA) assay kit. The proteins were separated by 10 % SDS-PAGE gels and transferred onto polyvinylidene difluoride (PVDF) membranes. Membranes were blocked with Tris buffered saline-Tween-20 containing 5 % non-fat milk and incubated overnight at

4℃ with primary antibodies for SR-A, CD 68 and β-actin. Then, the membranes were incubated with secondary antibodies conjugated with horseradish peroxidase for 1 h. The targeted protein was detected by a CLiNX-6300 imaging system (Clinx Science Instruments Co., Ltd., Shanghai, China) and quantified by AlphaEase FC software (open source). All reagents were provided by Wuhan Servicebio Technology Co., Ltd. (Wuhan, Hubei, China).

Sample Preparation Process for TEM

LPS-activated cells were grown on 60 mm culture dishes. Then, original medium was replaced by medium containing MPmTN at a concentration of 0.5 mg/mL. After incubation for 4 h, the remaining MPmTN was washed off with PBS. The cells were collected by centrifugation for 5 min at 1 000 rpm and fixed with 0.5 % (v/v) glutaraldehyde for 10 min at 4 ℃. Subsequently, the cells were rinsed at 12 000 rpm for 10 min. The supernatant was discarded. The precipitated cells were fixed with 3 % (v/v) glutaraldehyde and refixed with 1 % osmium tetroxide. The samples were dehydrated by an ascending series of acetone (30 %, 50 %, 70 %, 80 %, 90 %, 95 % and 100 %) and embedded in epoxy resin. Thin slices (50 nm) of the pellet were made and stained with uranyl acetate and lead citrate. Finally, the slices were observed under TEM (JEM-1400 PLUS, Japan Electronics Co., LTD., Japan) and photographed.

***In Vitro* Production of Blood Clots**

As in a previous study [6], 10 mL of fresh arterial blood was obtained from the marginal ear arteries of New Zealand White rabbits (n=6 total, female, 2.5 Kg body weight) by means of needle puncture and incubated in a water bath at a temperature of 37 ℃ for 4 h. Then the clot formed and be cut into small cubes (each $1 \times 0.2 \times 0.3$ cm, weighing approximately 200 mg). Blood clots were carefully washed three times with PBS solution and ready for further use.

CCK8 for Cytotoxicity Test

The cytotoxicity of MPmTN as well as the Fe-PFP-PLGA NPs *in vitro* was evaluated using CCK8 test for human umbilical vein endothelial cell (HUVEC), activated and unactivated RAW 264.7 cells. The cells were seeded into 96-well plates and incubated for 24 h. Then, original medium was replaced with 100 μL of medium containing MPmTN or the Fe-PFP-PLGA NPs at a series concentration of 0, 0.5, 1, 2, 3, 4 mg/mL. After incubation for 24 h, the cells were washed three times with PBS. Subsequently, 10 μL of CCK8 solution was added and incubated at 37 °C. The absorbance of the solution in each well was measured at 450 nm on a microplate reader (Synergy Mx, BioTek Instruments, Inc., Winooski, VT, USA). Untreated cells in growth medium were used as the control groups (containing cells, medium, CCK8 agents), and the wells without cells were used as blank groups (containing medium, CCK8 agents). The cell viabilities (%) were calculated through the following the formula, refer to the instruction:

$$Cell\ viability = \frac{(As - Ab)}{(Ac - Ab)} \times 100\ \%$$

In this formula, As was the absorbance resulting from experimental group, and Ac and Ab represented the absorbance of control group and blank group, respectively.

Hemolysis Test

A hemolysis test was carried out to evaluation the safety of MPmTN *in vitro* [7, 8]. 2 % red blood cell solutions were obtained from extracted for fresh whole blood samples collected with EDTA-coated tubes, after centrifugation at 1 000 g, 4 °C for 10 min and diluted to 50-fold with PBS. Then 0.5 mL cells were mixed with 0.5 mL of MPmTN at a series concentration of 0.5, 1, 2, 3 mg/mL. After incubation for 3 h at room temperature, the mixtures were centrifuged at 1 000 g for 10 min, and the absorbance of supernatant was measured on a microplate reader mentioned above at 570 nm. The hemolysis ratio was calculated. Cells mixed with 0.5 mL double-distilled water or PBS was used as positive or negative control, respectively. The hemolysis ratio was calculated based on the formula:

$$Hemolysis\ Ratio = \frac{A_s - A_N}{A_P - A_N} \times 100\ \%$$

In this formula, As was the absorbance resulting from experimental group, and A_P and A_N represented the absorbance of positive and negative groups, respectively.

Biosafety and Pharmacokinetic Study in vivo

ApoE-/- mice with a western diet for 16 weeks and normal age-matched mice with a normal diet were used for the biosafety study of NPs. 1 week adapted to the environment, two types of mice were divided into three groups (n=3/group) and injected with 200 μL of PBS, the Fe-PFP-PLGA NPs or MPmTNs at 1 mg/mL via the tail vein, respectively. The mice were observed closely to detect signs of irritation, pain, discomfort, or inflammation. 7 days after the administration, the heart, liver, spleen, lung, and kidney were harvested and fixed with 4 % paraformaldehyde for H&E staining.

For pharmacokinetic study of NPs in vivo, ApoE$^{-/-}$ mice fed a western diet for 16 weeks were administered 200 μL of 1 mg/mL MPmTNs via the tail vein. 100 μL of blood samples were collected from eye socket at indicated time points of 2 min, 30 min, 4 h, 8 h and 24 h. Then, the blood samples were dissolved in digestive chloroazotic acid (V_{HCl}/V_{HNO3}=1/3) to quantify the content of Fe using ICP. Fe was used as a marker for dynamic monitoring of the blood concentration of MPmTNs.

2. Supplementary Table and Figures

Table S1. Characteristics of different NPs (n=3)

Sample	ζ potential (mV)	Diameter (nm)	Polydispersity Index (PDI)
Fe-PFP-PLGA	-21.42 ± 0.40	270.13 ± 1.60	0.073 ± 0.015
Fe-PFP-PLGA@PP1	-20.26 ± 0.68	299.13 ± 1.93	0.149 ± 0.033
Fe-PFP-PLGA@cRGD	-18.39 ± 0.67	296.77 ± 2.24	0.158 ± 0.021
Fe-PFP-PLGA@PP1-cRGD	-34.90 ± 0.85	289.54 ± 1.69	0.186 ± 0.020
Fe-PLGA	-25.74 ± 0.53	220.17 ± 1.43	0.106 ± 0.030
Fe-PLGA@PP1-cRGD	-34.29 ± 0.57	222.15 ± 1.72	0.141 ± 0.029
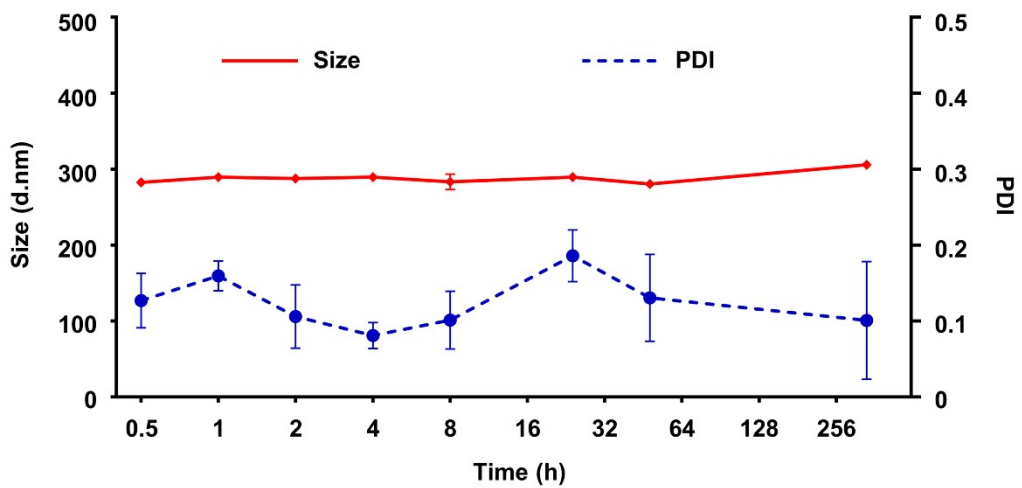
Figure S1. Time-dependent particle size and PDI variances of MPmTN at 25 ℃.
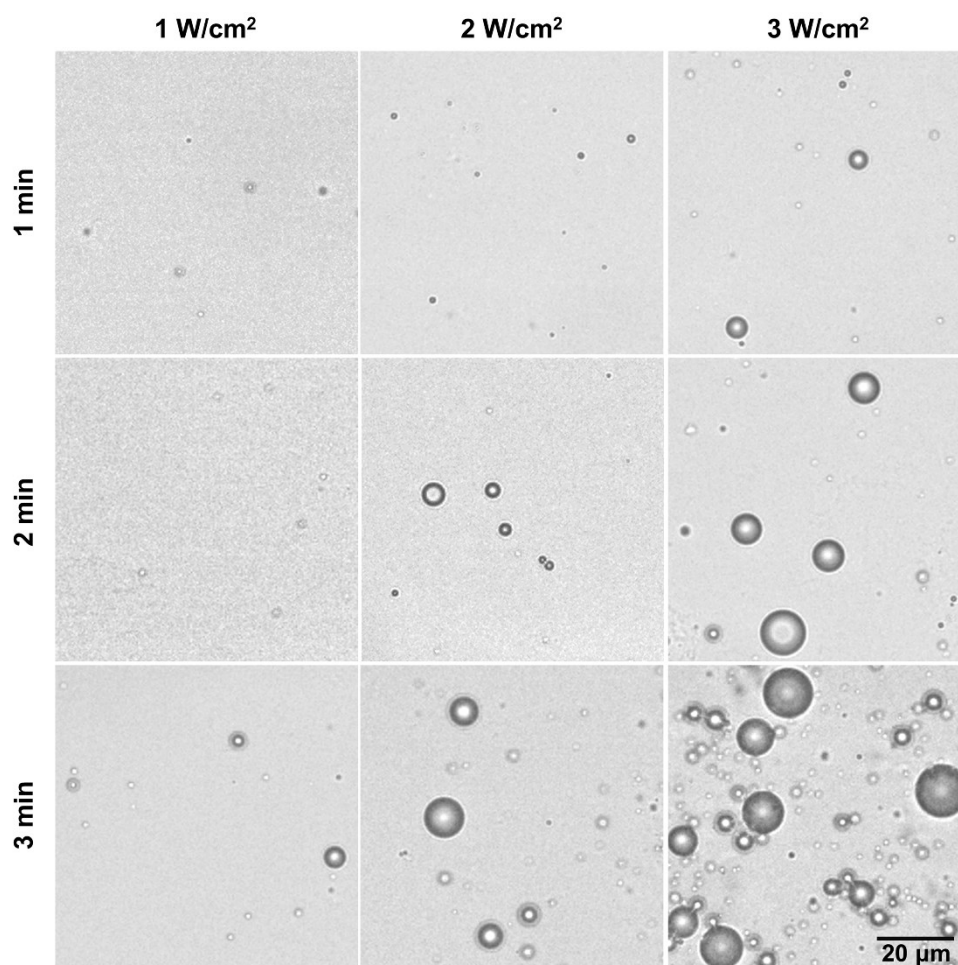
Figure S2. Optical microscopy images of MPmTN after ultrasonic treatment at power densities of 1,2 and 3 W/cm² for 1, 2 and 3 min, 3 MHz and 30 % duty cycle.
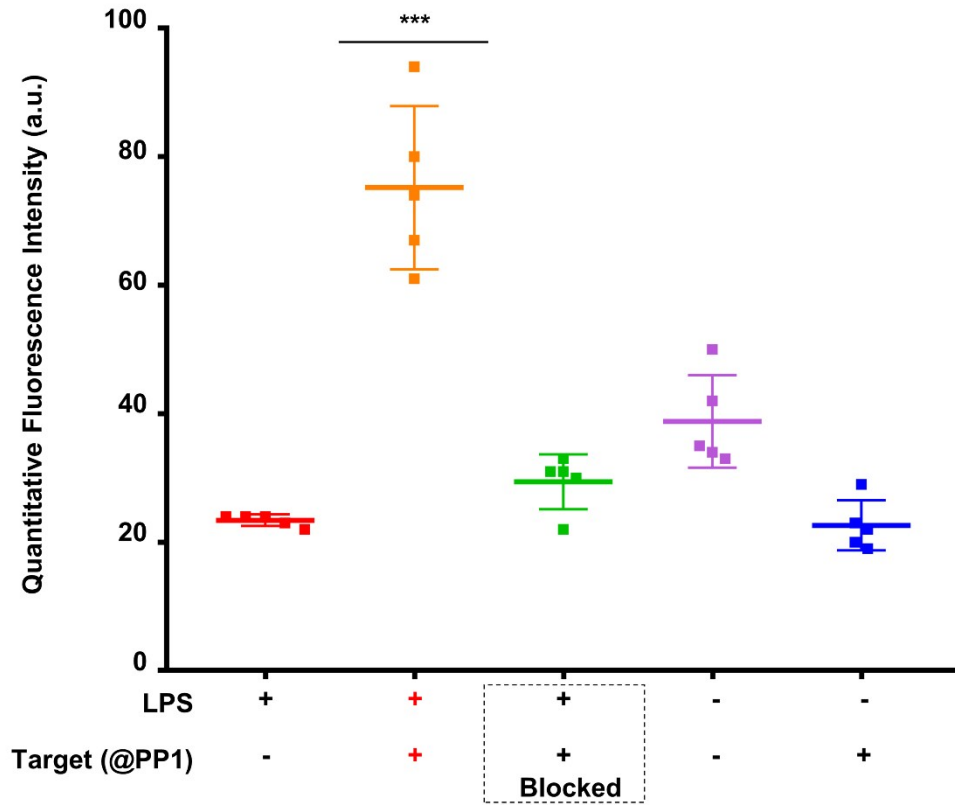
Figure S3. Quantitative fluorescence intensity of CLSM images (Figure 4D) of macrophages after incubation with NPs. LPS (+): activated macrophages; LPS (-): unactivated macrophages; Targeted (@PP1) (+): the Fe-PFP-PLGA@PP1-cRGD NPs; Targeted (@PP1) (-): the Fe-PFP-PLGA@cRGD NPs; Blocked: excess PP1 solution incubated with cells before the NPs.
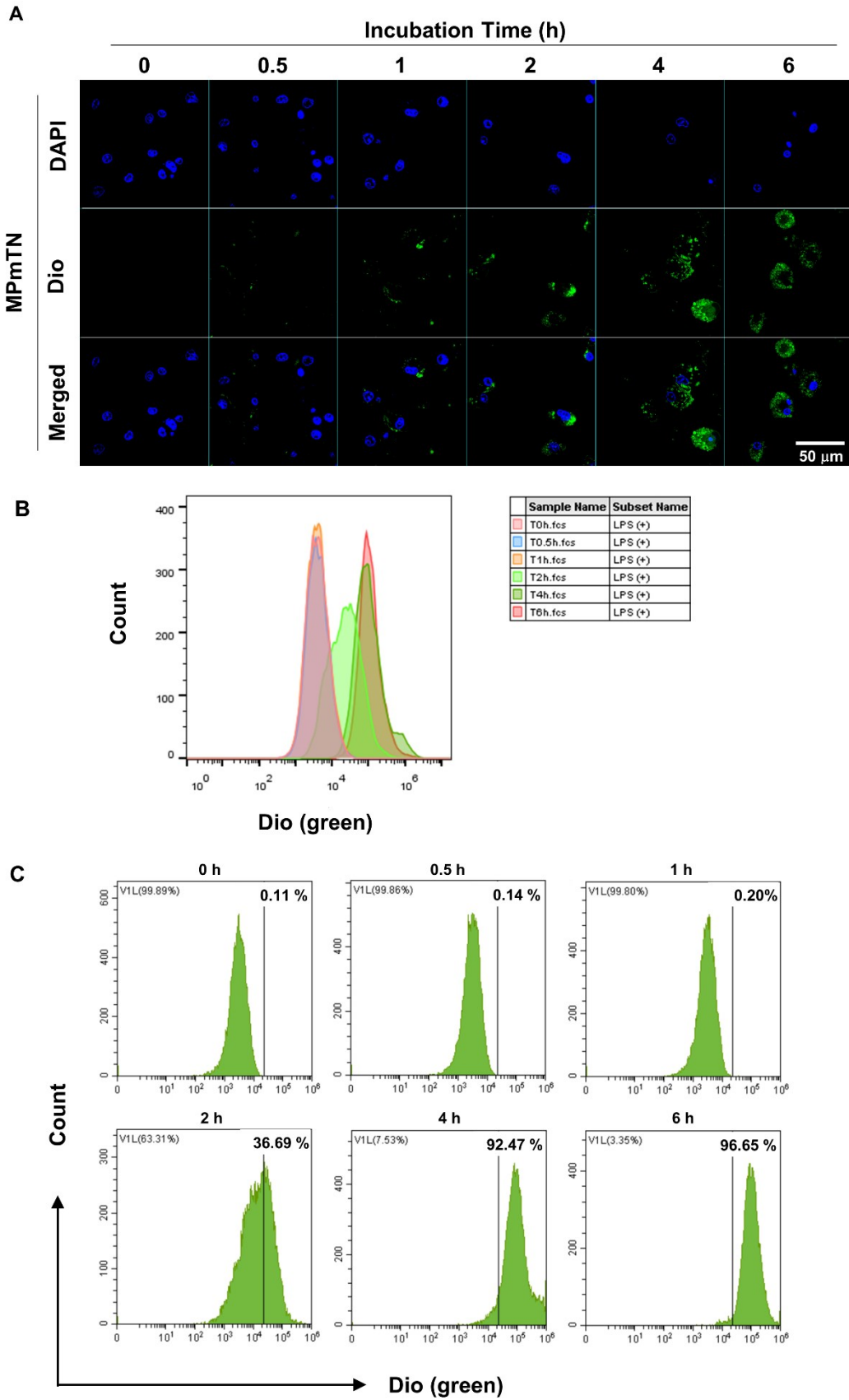
Figure S4. Time-point study of the Dio-labeled MPmTN **(green)** towards LPS-

activated macrophages using (A) CLSM, (B) FCM and (C) quantitate analysis of FCM. The nucleus was stained by DAPI **(blue)**.
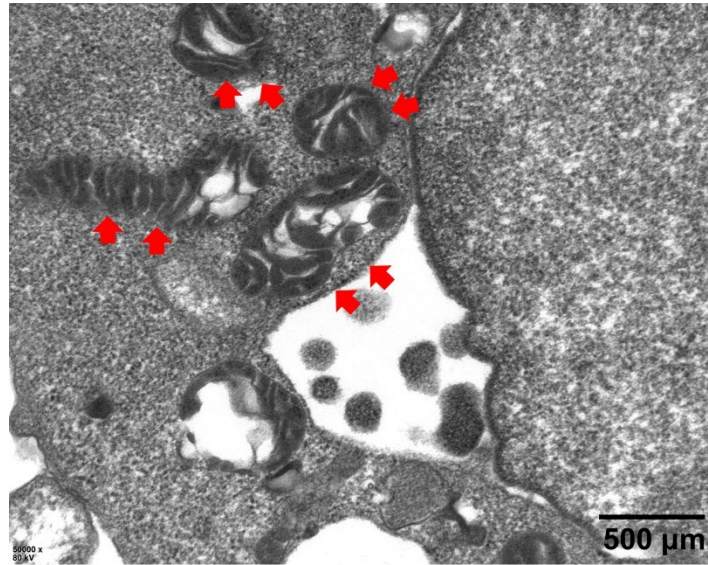
Figure S5. TEM images of the LPS-activated macrophages after treatment in the US + PFP group. Typical morphologic characteristics of swollen mitochondria were shown (red arrow)**.**
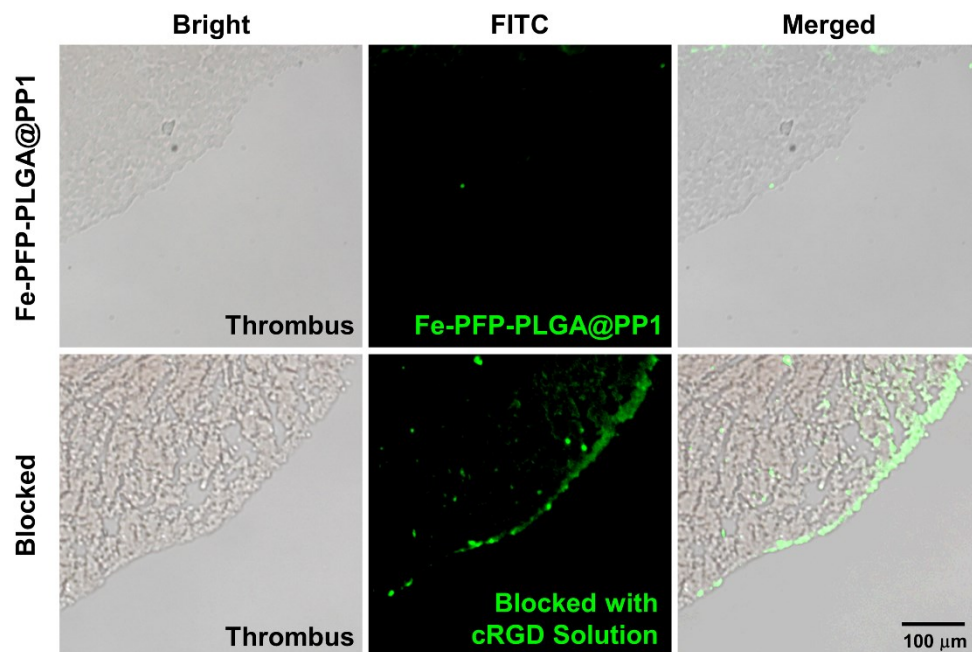
Figure S6. *In vitro* binding assay of blood clots incubated with the Dio-labeled Fe-PFP-PLGA@PP1 NPs **(green)**, and Dio-labeled MPmTN **(green)** after the blocking of cRGD solution.
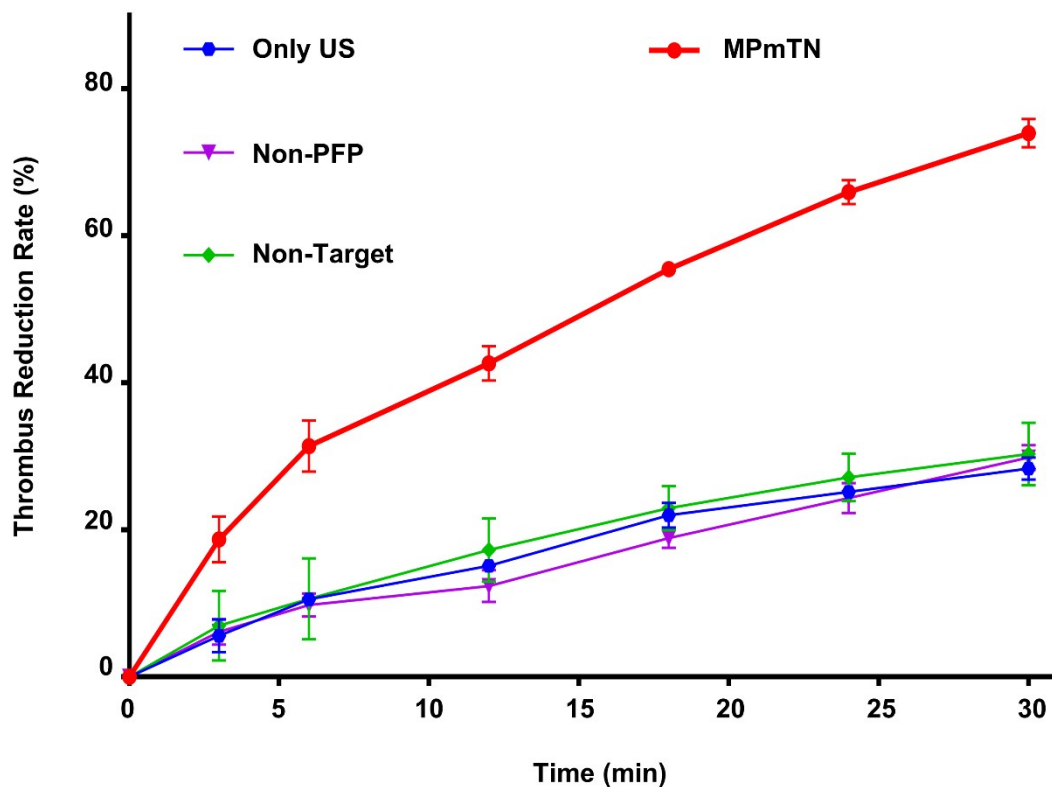
Figure S7. The thrombus reduction rate of blood clots varies at different time points over a 30 min period of US irradiation exposure under 3 W/cm^2. Blood clots were divided into four groups and placed in PBS, the Fe-PLGA@PP1-cRGD or Fe-PFP-PLGA@PP1 NPs, MPmTN separately (Simplified as Only US, Non-PFP, Non-Target, MPmTN).
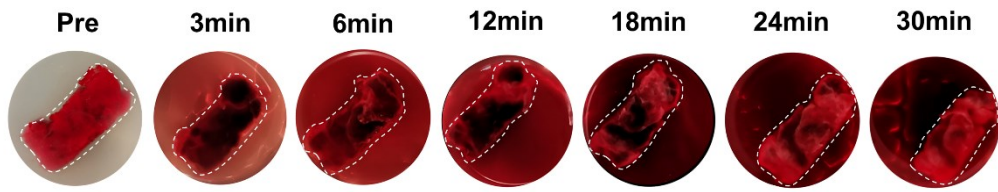
Figure S8. The gross appearance of blood clots incubated with MPmTN in the agarose model under US exposure at a power of 3 W/cm^2 for different time points.
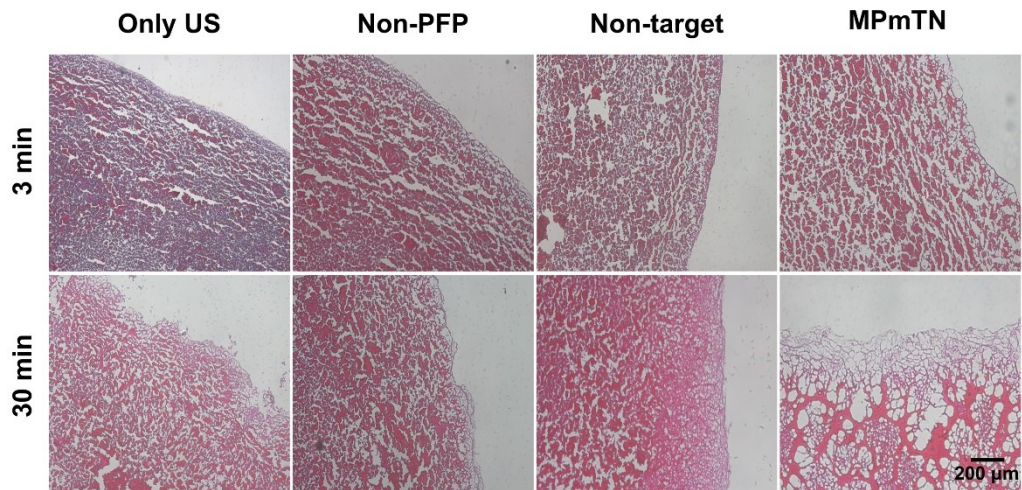
Figure S9. Representative H&E staining of blood clots in different groups under US treatment at a power of 3 W/cm² for 3 min or 30 min. Blood clots were divided into four groups and placed in PBS, the Fe-PLGA@PP1-cRGD NPs or the Fe-PFP-PLGA@PP1 NPs, MPmTN separately (Simplified as Only US, Non-PFP, Non-Target, MPmTN).
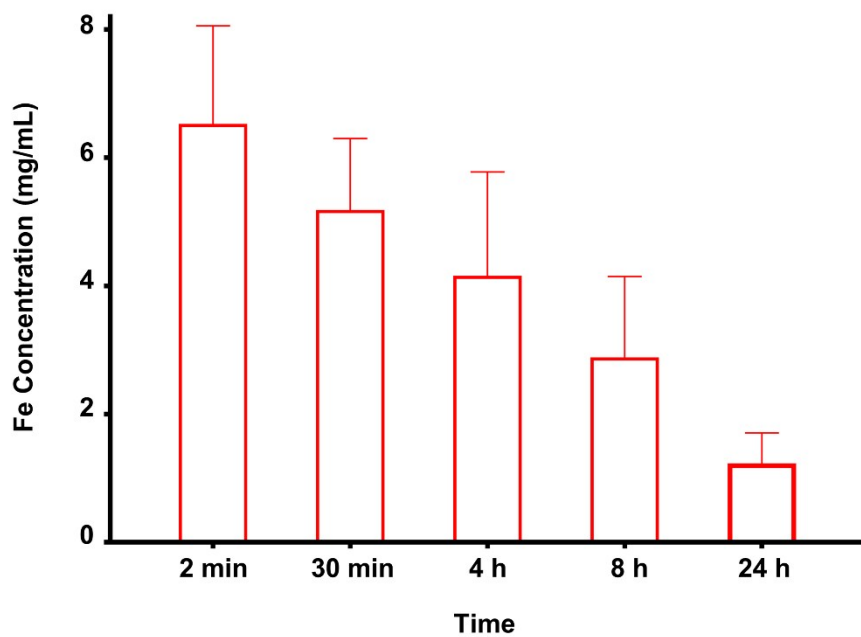
Figure S10. *In vivo* pharmacokinetic performance of MPmTN after *i.v.* injection in mice. Fe concentration was measured using ICP, as the marker of Fe-containing MPmTN.
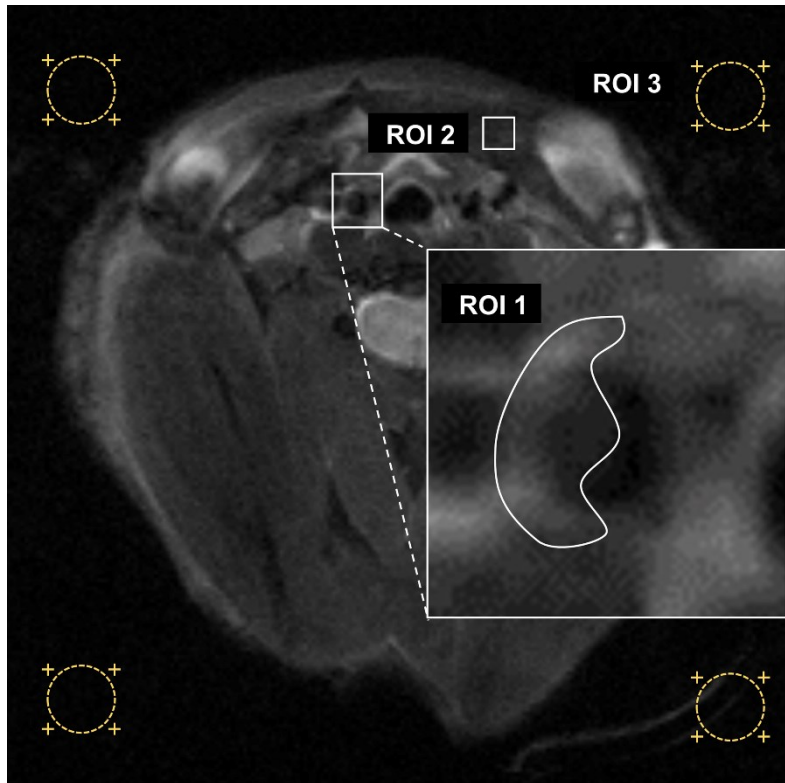
Figure S11. CNR of atherosclerotic plaques were determined by a cross-section of the blood vessel in T_2-weighted images. The signal intensity of the plaque in the vessel wall (I_{wall}) was measured in ROI 1, and corrected by ROI 2 (I_{muscle}) and ROI 3 ($stdev_{noise}$). The atherosclerotic plaque area was outlined as ROI 1, surrounding muscle tissue was selected as ROI 2 and the SD of the noise ($stdev_{noise}$) was calculated by the signal intensity of ROI 3.
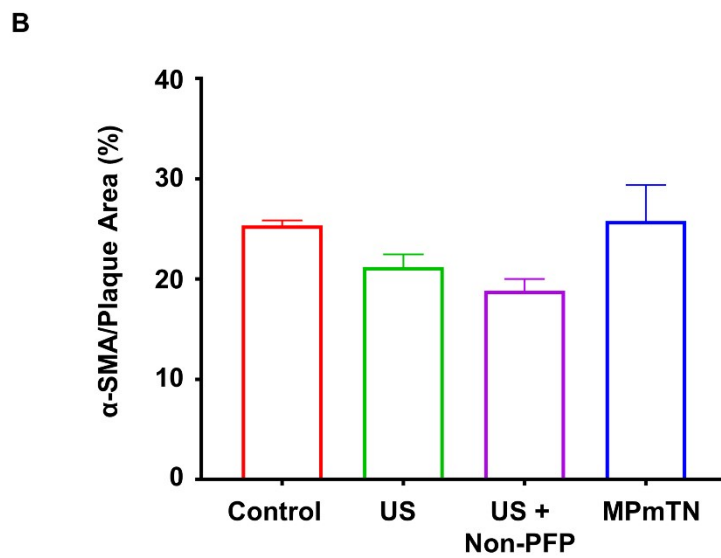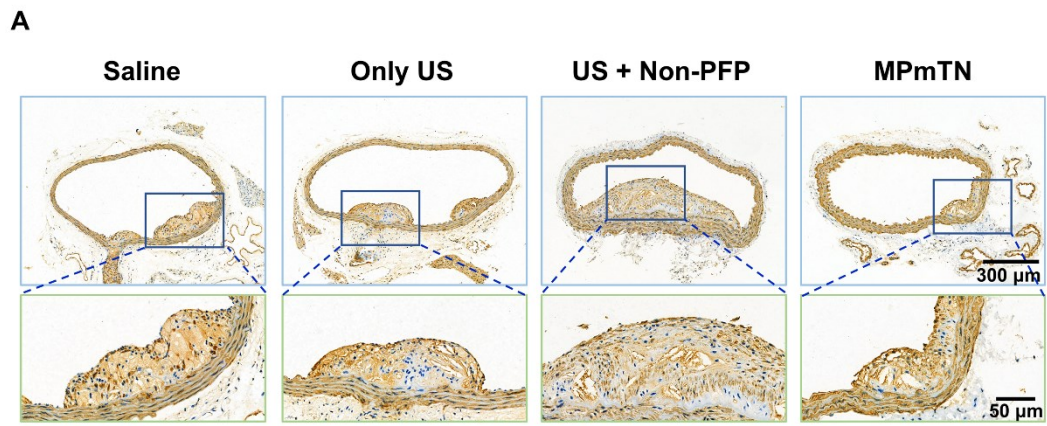
A

B

Figure S12. (A) Representative images of aortic root sections stained with antibody of α-SMA, and (B) quantitative analysis of plaque α-SMA area relative to plaque area.
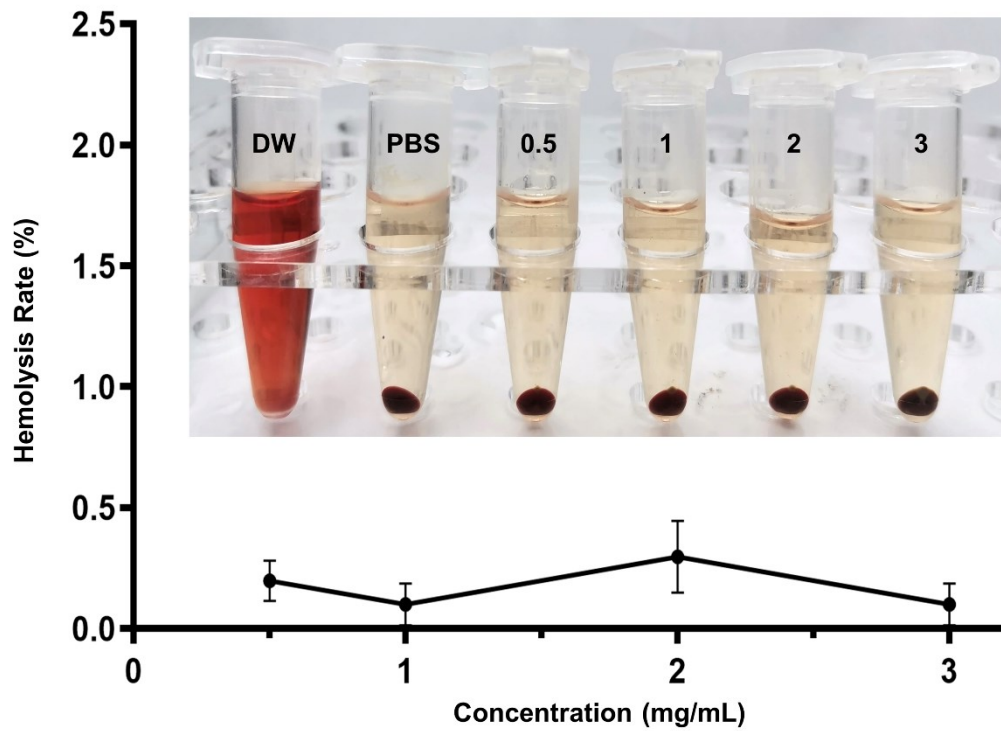
Figure S13. Biocompatibility of the as-fabricated MPmTN at different concertation of 0.5, 1, 2, 3 mg/mL via *in vitro* hemolysis test. Picture inset showing the corresponded hemolysis images of positive control (deionized water, DW) and NPs at different concentration and negative control (PBS), respectively.
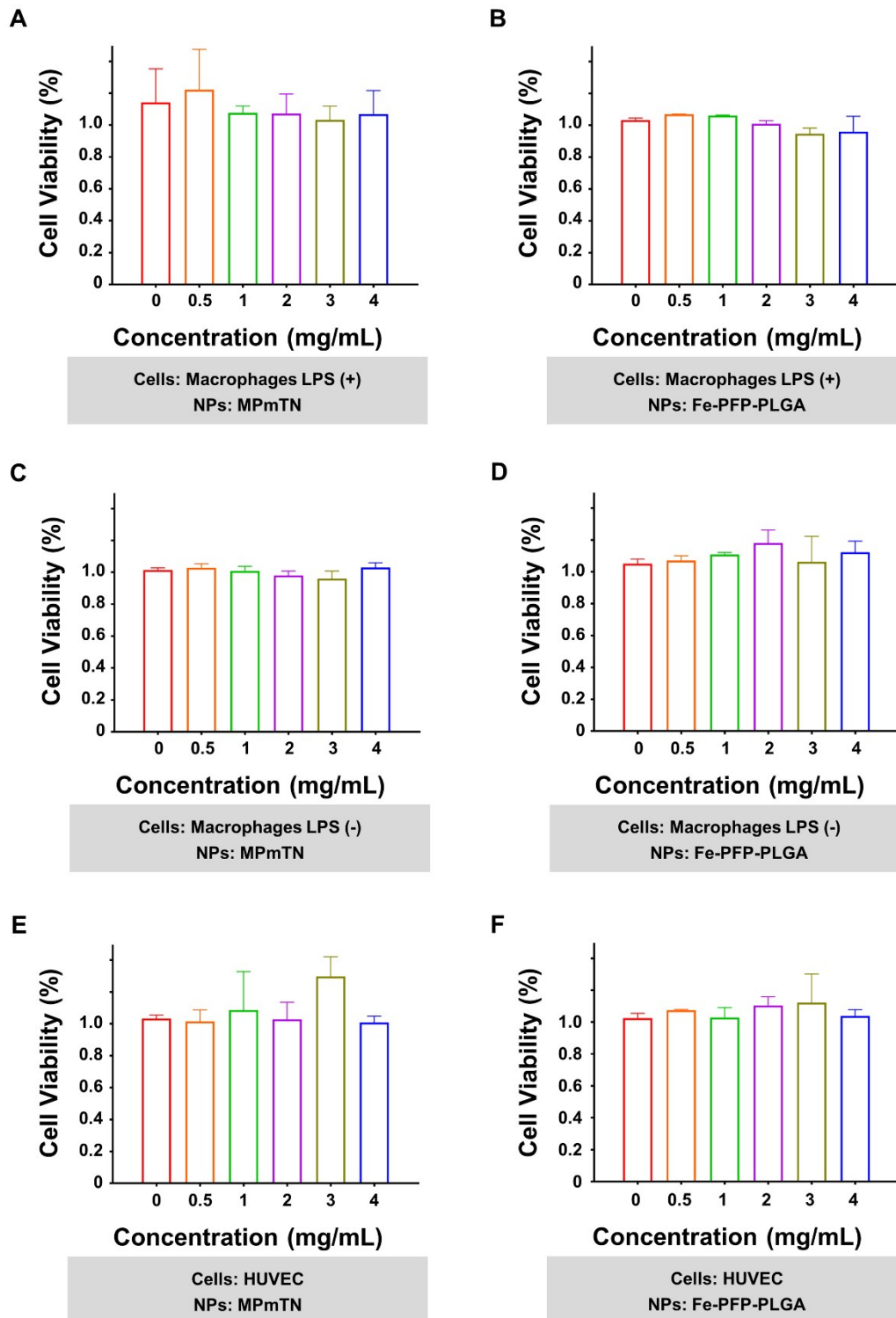
Figure S14. *In vivo* cytotoxicity evaluation of MPmTN or the Fe-PFP-PLGA NPs in different cells. Cell viability values of LPS-activated macrophages after incubation with various doses of (A) MPmTN or (B) the Fe-PFP-PLGA NPs for 24 h. Cell viability values of unactivated macrophages after incubation with various doses of (C) MPmTN

or (D) the Fe-PFP-PLGA NPs for 24 h. Cell viability values of human umbilical vein endothelial cells (HUVEC) after incubation with various doses of (E) MPmTN or (F) the Fe-PFP-PLGA NPs for 24 h.
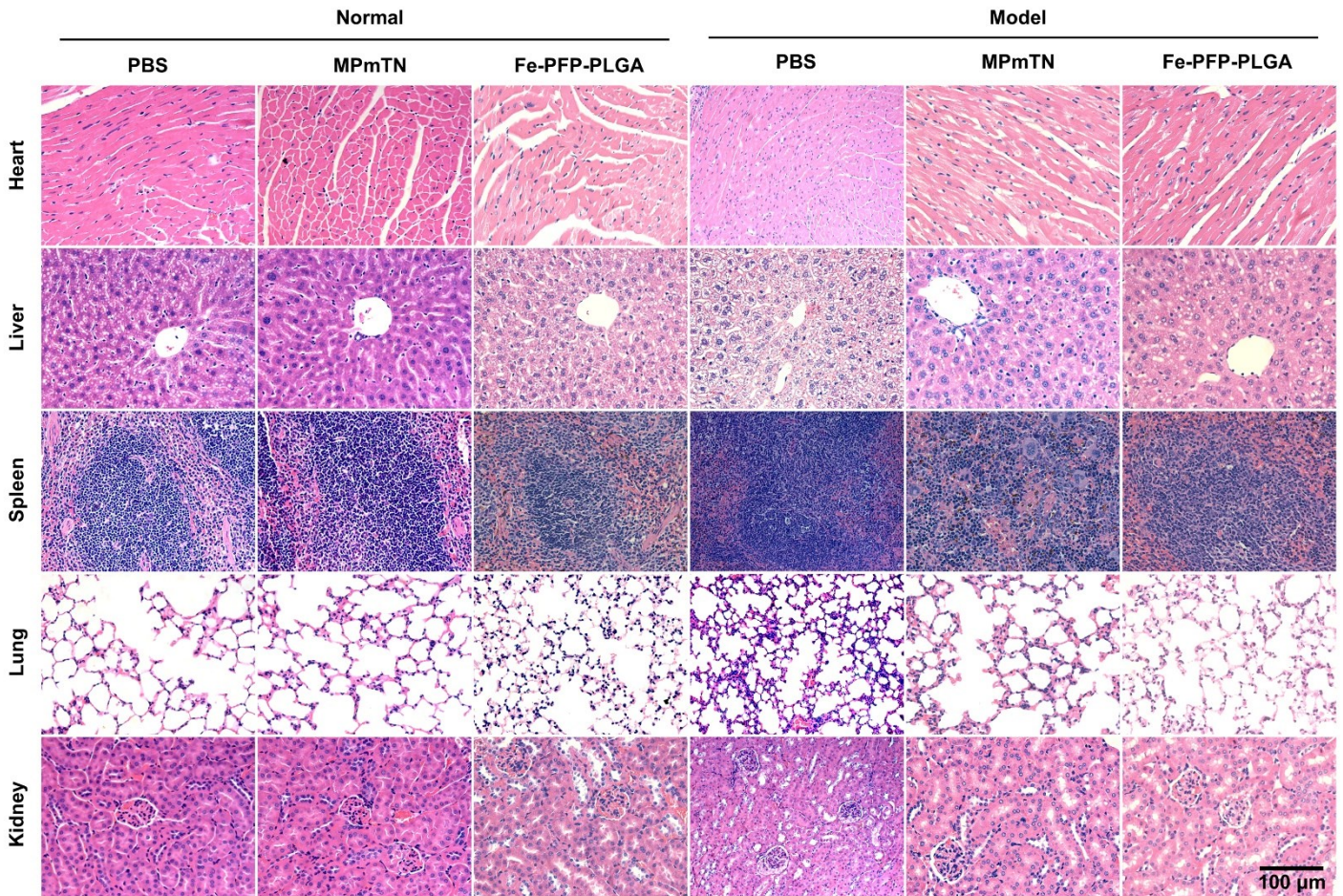

Figure S15. H&E stained sections of major organs. Normal groups used age-match C57BL/6J mice fed with normal diet. Model groups used apoE$^{-/-}$ mice fed a cholesterol-rich high-fat diet for 16 weeks. Mice in the PBS group were treated with PBS alone by *i.v.* injection, while other groups were separated administered with 200 µL of 1 mg/mL MPmTN or the Fe-PFP-PLGA NPs via the tail vein. Organs including heart, liver, spleen, lung, and kidney were resected after 7 days of different treatments.

References

1   A.S. Guedj, A.J. Kell, M. Barnes, S. Stals, D. Goncalves, D. Girard, C. Lavigne, *International journal of nanomedicine*, 2015, 10, 5965-79.

2   Y.S. Kim, J.S. Park, M. Park, M.Y. Ko, S.W. Yi, J.A. Yoon, S. Yang, S.H. Shim, K.H. Park, H. Song, *Biomaterials*, 2018, 183, 43-53.

3   G.Y. Lee, J.H. Kim, K.Y. Choi, H.Y. Yoon, K. Kim, I.C. Kwon, K. Choi, B.H. Lee, J.H. Park, I.S. Kim, *Biomaterials* 2015, 53, 341-8.

4   J. Li, Y. He, W. Sun, Y. Luo, H. Cai, Y. Pan, M. Shen, J. Xia, X. Shi, *Biomaterials*, 2014, 35(11), 3666-77.

5   C.A. Schneider, W.S. Rasband, K.W. Eliceiri, *Nature Methods*, 2012, 9(7), 671-675.

6   J. Xu, J. Zhou, Y. Zhong, Y. Zhang, J. Liu, Y. Chen, L. Deng, D. Sheng, Z. Wang, H. Ran, D. Guo, *ACS applied materials & interfaces*, 2017, 9(49), 42525-42535.

7   J. Xu, X. Cheng, L. Tan, C. Fu, M. Ahmed, J. Tian, J. Dou, Q. Zhou, X. Ren, Q. Wu, S. Tang, H. Zhou, X. Meng, J. Yu, P. Liang, *Nano letters*, 2019, 19(5), 2914-2927.

8   D. Long, T. Liu, L. Tan, H. Shi, P. Liang, S. Tang, Q. Wu, J. Yu, J. Dou, X. Meng, *ACS nano*, 2016, 10(10), 9516-9528.